CHAPTER V

RESULTS AND DISCUSSION

In preliminary experiments, the study was conducted so as to investigate the physical and chemical properties of Ag/Al_2O_3 and Pt/Al_2O_3 catalyst in various alumina phases. The Al_2O_3 supports were synthesized by solvothermal technique. Various χ/γ phase composition ratios were adjusted as 0/100, 10/90, 30/70, 50/50, 70/30 and 100/0. The catalytic properties were evaluated using selective catalytic reduction of NO, carbon monoxide oxidation and selective carbon monoxide oxidation in excess hydrogen. The results in this chapter are divided into four main parts. The first part describes the characteristics of alumina consisting of various phase compositions between gamma and chi alumina (section 5.1). The second part describes the catalytic properties and activities of Ag/Al_2O_3 in selective catalytic reduction of NO by propane under lean-burn condition (section 5.2). The others part describe the catalytic properties and activities of Pt on gamma and chi alumina supports in CO oxidation (section 5.3) and the catalytic properties and activities of Pt on gamma and chi alumina supports in selective CO oxidation (section 5.4).

5.1 The properties of alumina supports

5.1.1 X-ray diffraction pattern

Bulk crystal structure and chemical phase composition of a crystalline material can be detected by diffraction of an X-ray beam as a function of the angle of the incident beam. The measurements were carried out at the diffraction angles (2θ) between 20 and 80 degrees. Broadening of the diffraction peaks was used to estimate crystallite diameter from Scherrer Equation as shown in Appendix A.

Alumina supports were prepared by the solvothermal synthesis. The gamma and chi phases were produced using the different solvent precursor, i.e. 1-butanol and toluene, respectively. Various chi/gamma phase compositions were controllably obtained by

mixing 1-butanol and toluene in an appropriate ratio. XRD pattern of the alumina supports is shown in Figure 5.1. For the pure gamma phase, XRD peaks at 32°, 37°, 39°, 45°, 61° and 66° were evident. When adding toluene in 1-butanol, XRD peaks were appeared at 37°, 40°, 43°, 46°, 60°, and 67°. The peak at 43° was dominant. This peak showed characteristics of the chi phase and thus the increase of chi alumina phase leaded to larger peak area at 43°. Certainly, the pure gamma alumina did not show the peak area at 43°. The results were in agreement with the work previously reported about the effect of solvent on the preparation of alumina [166]. In this work, the alumina samples consisting of 0, 10, 30, 50, 70 and 100% chi phase were named as C0G100, C10G90, C30G70, C50G50, C70G30 and C100G0, respectively. The phase compositions of alumina supports were determined by area of chi major peak (43°) from XRD pattern. The calibration curve of this peak was obtained by varying the ratio of pure gamma and pure chi alumina in the physical mixtures as shown in Figure 5.2. Therefore, we can calculate % chi phase in sample from this calibration curve. The calculation method gave an error in a range of $\pm$ 10%.

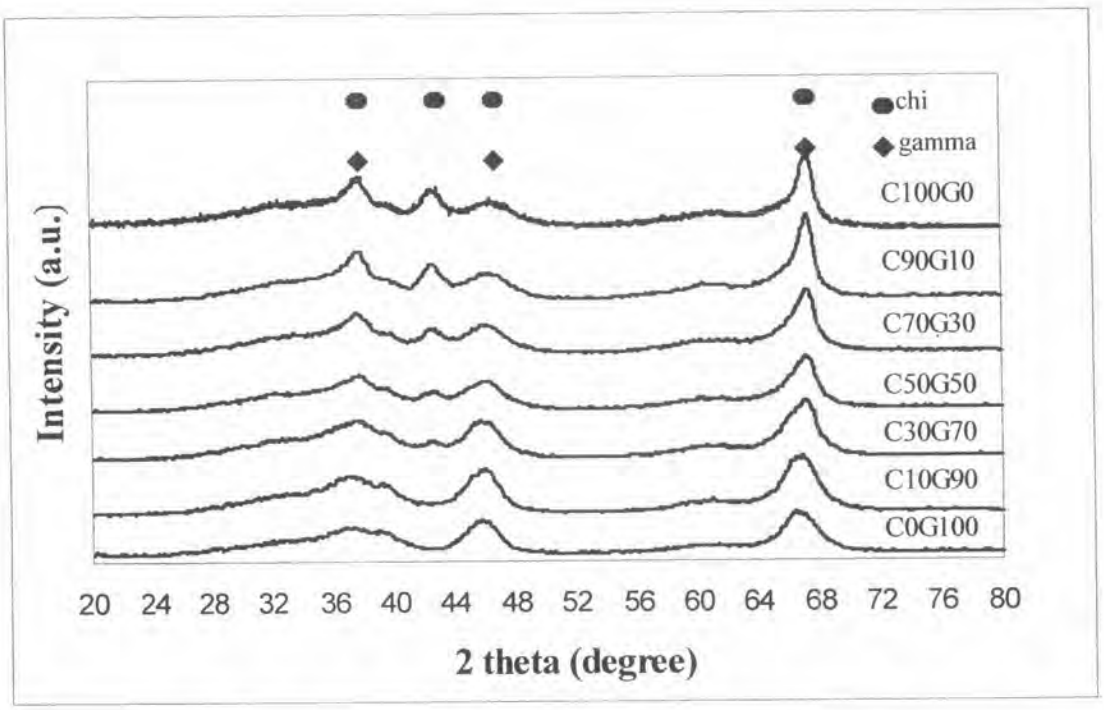

Figure 5.1 X-ray diffraction pattern of alumina supports

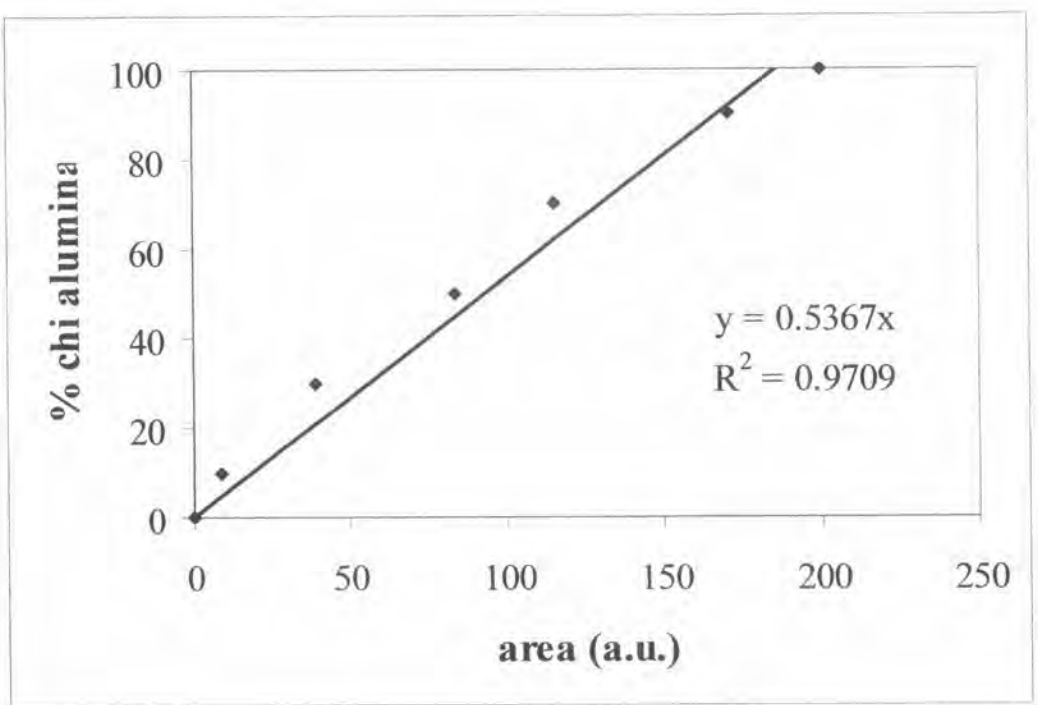

Figure 5.2 The calibration curve of %chi alumina phase

5.1.2 The physical properties

The physical properties of the alumina supports are summarized in table 5.1. The BET surface area decreased slightly when the chi phase was in the alumina structure. The pure gamma and pure chi phases showed 226 and 168 m^2/g, respectively. The average pore diameter was rather similar for the different ratio of phase composition.

Table 5.1 The physical properties of alumina supports

Sample	Crystallite Size* (nm)	BET surface area (m^2g^{-1})	Pore Volume ($cm^3.g^{-1}$)	Avg. Pore Diameter (nm)
C0G100	5	226	0.63	8
C10G90	5	213	0.50	8
C30G70	5	203	0.53	9
C50G50	6	182	0.44	7
C70G30	6	177	0.42	6
C100G0	6	168	0.57	9

* Calculate from XRD

5.1.3 Scanning electron microscopy (SEM)

SEM was performed to study the morphologies of alumina supports. That significant change was found in morphologies upon phase composition. A typical SEM micrograph for alumina supports are shown in Figure 5.3(a) - 5.3(f). The gamma alumina showed the whicker sheet structure but the chi alumina showed the spherical structure.

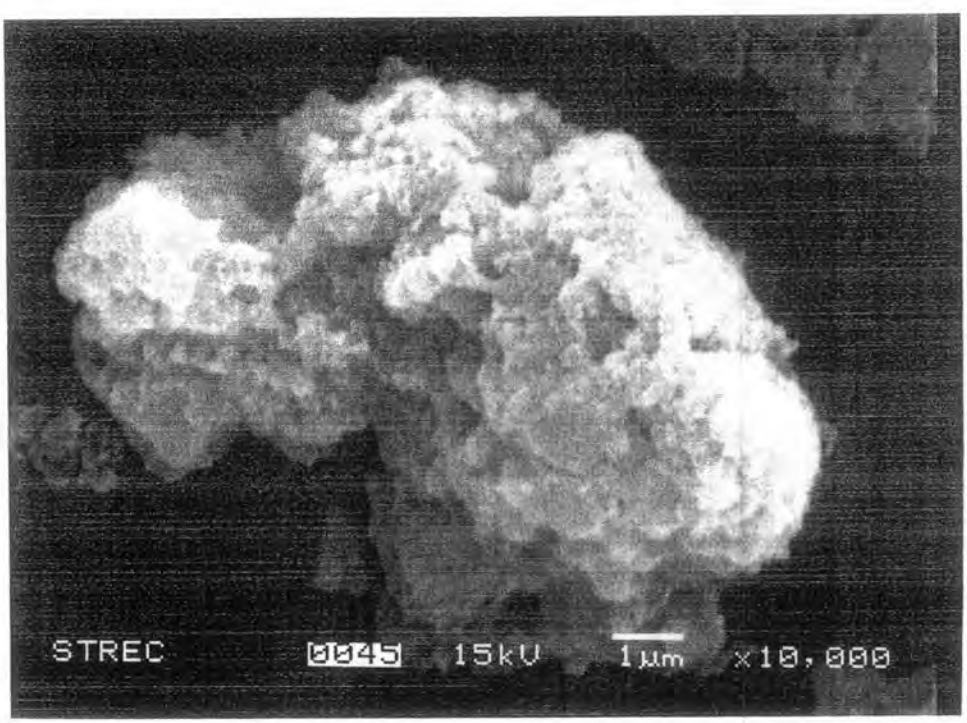

Figure 5.3(a) SEM micrograph of C0G100

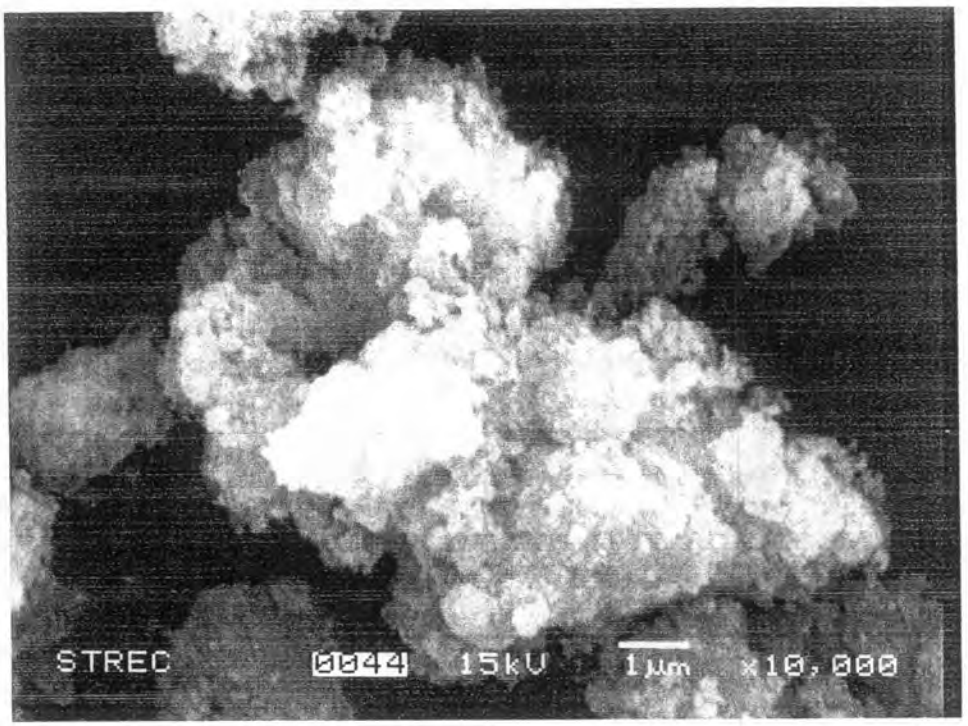

Figure 5.3(b) SEM micrograph of C10G90

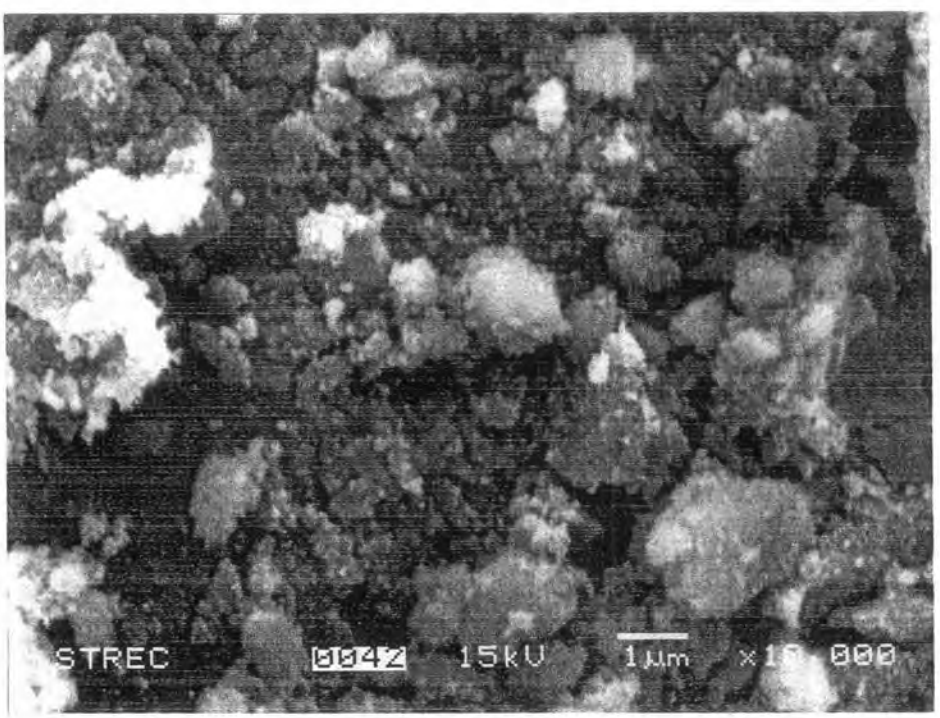

Figure 5.3(c) SEM micrograph of C30G70

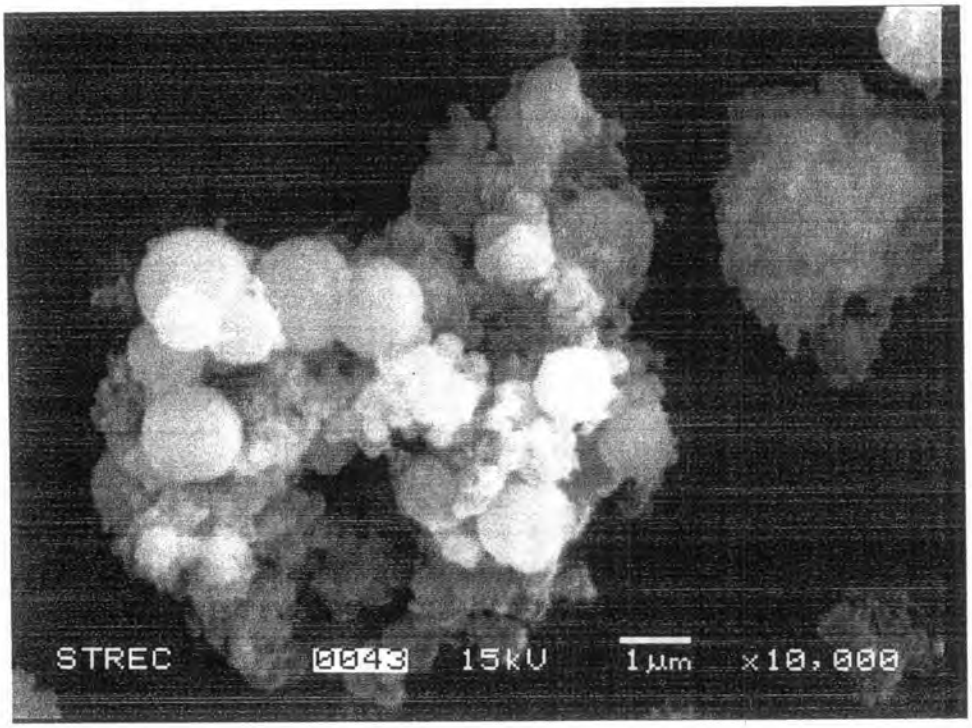

Figure 5.3(d) SEM micrograph of C50G50

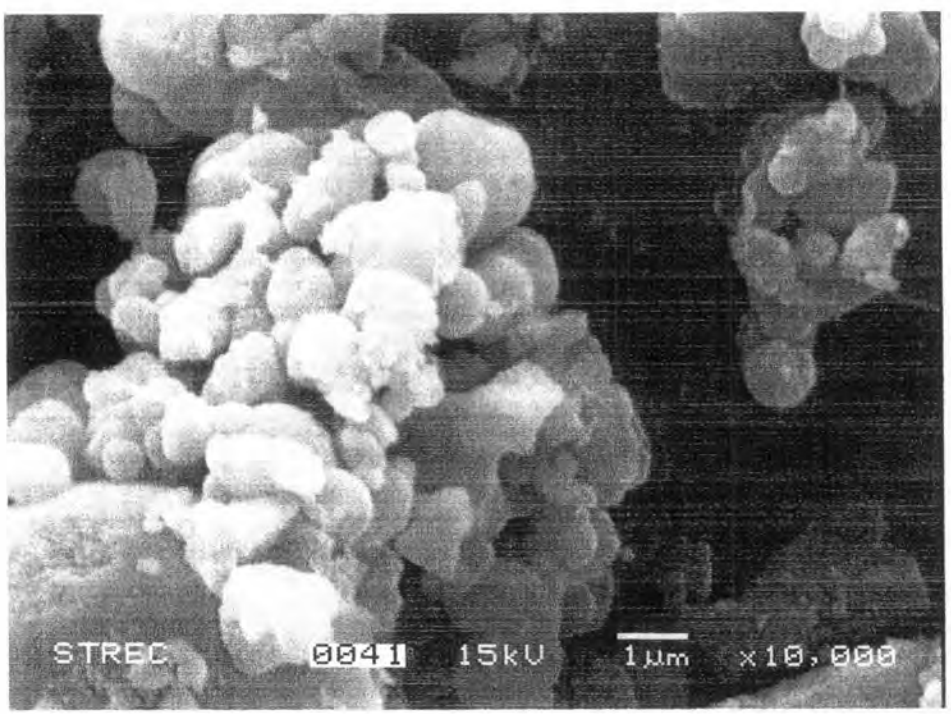

Figure 5.3(e) SEM micrograph of C70G30

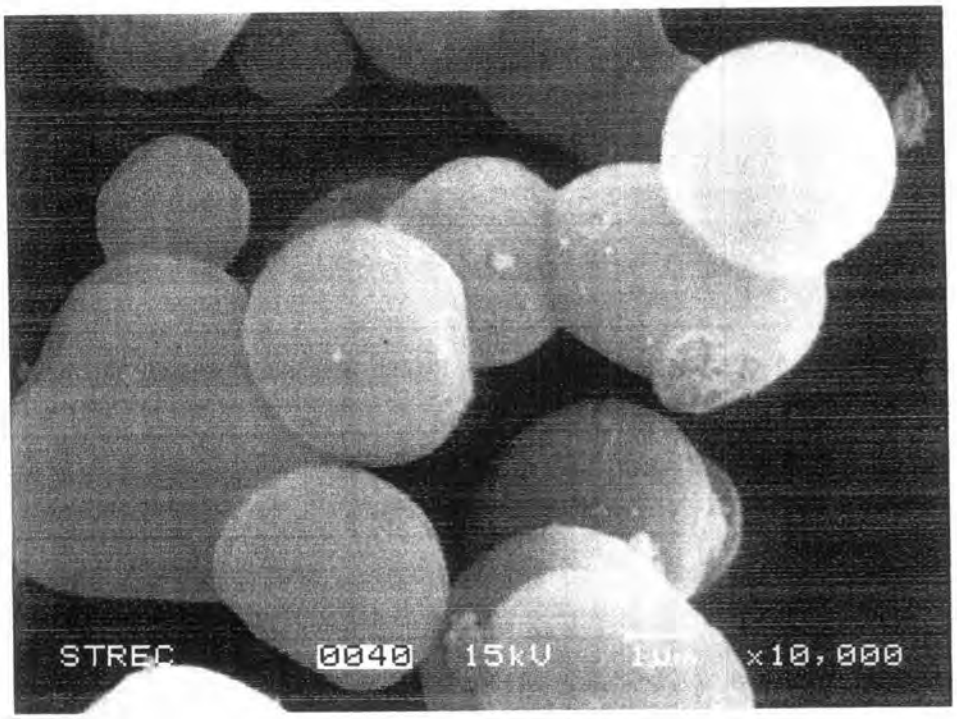

Figure 5.3(f) SEM micrograph of C100G0

5.1.4 Acidity behavior

In general, strong bases, as adsorbates, should in principle be suitable probes for the evaluation of the overall acidity of catalysts, as well as to distinguish between protonic (Brönsted) acidity and aprotic (Lewis) acidity. In this work, ammonia was independently used as probe molecules for acidity measurement. The total concentration of acid centers at the alumina supports was measured by ammonia temperature programmed desorption (NH_3-TPD) method. Although this procedure can not resolve to discriminate between different types of acid sites, it was routinely used to evaluate the total acidity of alumina supports. The spectra are reported in Figure 5.4. NH_3-TPD gave rise to a low temperature peak of gamma alumina, with a maximum point at 80°C. In mix phase, the increase of chi alumina phase affected the amount of acidity of alumina support. The NH_3 TPD curve of the pure chi phase showed a low temperature peak at 80°C and a broad high temperature peak at 200-300°C. Conclusively, the chi alumina phase has more strong acidity than gamma alumina phase.

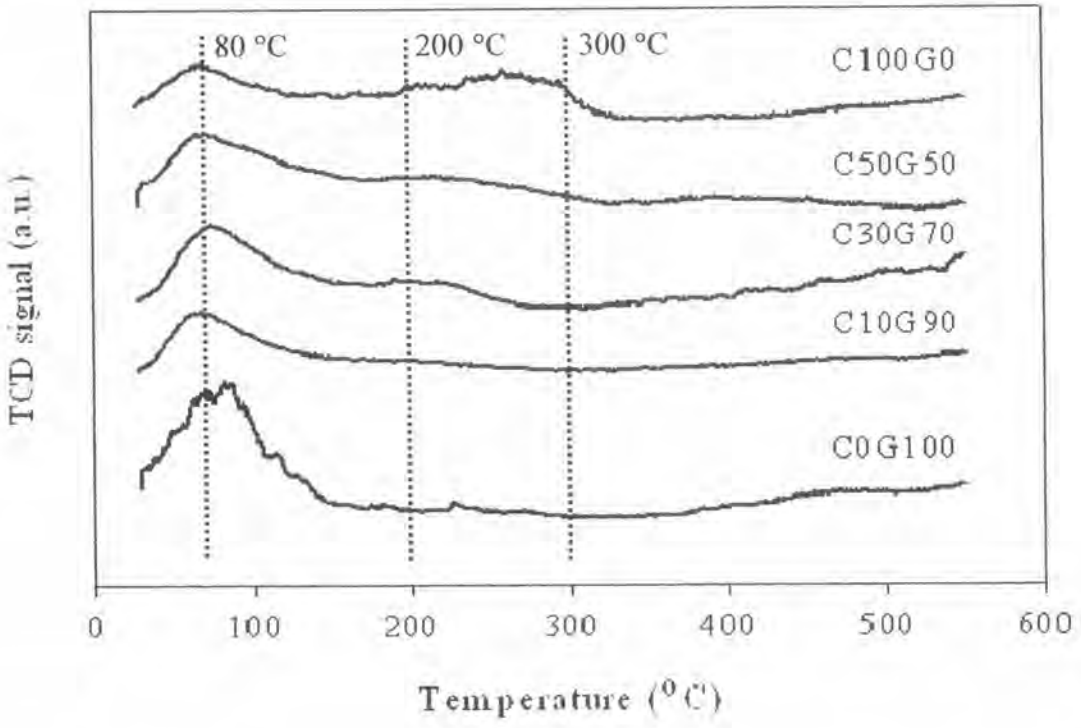

Figure 5.4 NH_3- temperature programmed desorption profiles of alumina samples

The acid properties of the alumina supports are also reported in table 5.2. The calculation of the acidity was shown in Appendix B. The acidity of pure gamma and pure chi alumina were 4.2 and 7.2 μmol NH_3/g catalyst, respectively. The acidity was increased from 4.2 to 9.8 μmol NH_3/g catalyst as the χ phase contents increased from 0 to 50 wt% and then decreased to 7.2 μmol NH_3/g catalyst as the χ phase contents increased further to 100 wt%. This result indicated that there were appropriate χ-phase contents for improving the acidity of γ-Al_2O_3 catalysts. The total acid concentration was improved in the following order: C50G50 > C100G0 > C10G90 > C30G70 > C0G100.

Table 5.2 Acidity of alumina supports

Alumina sample	Weak acidity[+] (μmol NH_3/g catalyst)	Strong acidity (μmol NH_3/g catalyst)	Acidity (μmol NH_3/g catalyst)	Acidity[*] (μmol/g catalyst)
C0G100	4.2	-	4.2	9
C10G90	5.8	0.8	6.6	13
C30G70	4.2	2.0	6.2	11
C50G50	6.5	3.3	9.8	19
C100G0	3.5	3.7	7.2	16

[*] Calculate from titration method

[+] Calculate from peak area at low temperature

5.2 Selective catalytic reduction of NO_x by propene

The influence of phase composition between gamma and chi alumina on Ag/Al_2O_3 catalysts in SCR of NO by propene was investigated in this section. The alumina with various phase compositions was used as the support of the silver catalyst. The silver was fixed as 2 wt% by incipient wetness impregnation.

5.2.1 Physical properties of 2 wt% Ag/Al_2O_3

The metal active sites of catalysts were measured by N_2O decomposition technique and related to Ag active surface dispersion. The results are given in table 5.3. The BET surface areas of Ag/Al_2O_3 were slightly less than those of the alumina supports. The metal active sites on the pure chi alumina and pure gamma alumina phase were rather equivalent at approximately 2.5×10^{19} molecule $N_2O\cdot(g\ catalyst)^{-1}$. The catalysts with mixed-phase alumina supports gave higher active sites than those with pure gamma and chi alumina except at 10 wt% chi phase.

Table 5.3 The catalyst properties of 2wt% Ag/Al_2O_3.

Sample	BET surface area ($m^2\cdot g^{-1}$)	Metal active sites $\times 10^{-19}$ (molecule $N_2O\cdot(g\ catalyst)^{-1}$)	% Ag dispersion (%)	Matel size* (nm)
Ag/C0G100	177	2.48	24	5
Ag/C10G90	166	1.93	19	6
Ag/C30G70	157	3.04	30	4
Ag/C50G50	135	3.06	30	4
Ag/C100G0	118	2.49	24	5

* Calculate from active sites

5.2.2 X-ray diffraction pattern

The XRD pattern of the catalysts is shown in the Figure 5.5. From the observation, the amount of the catalyst was fixed as 0.5 g in this experiment. The peaks of Ag^0 (2θ = 38.2 and 44.3°) in each sample were different. The 10 wt% chi phase showed the large size of metallic silver particle.

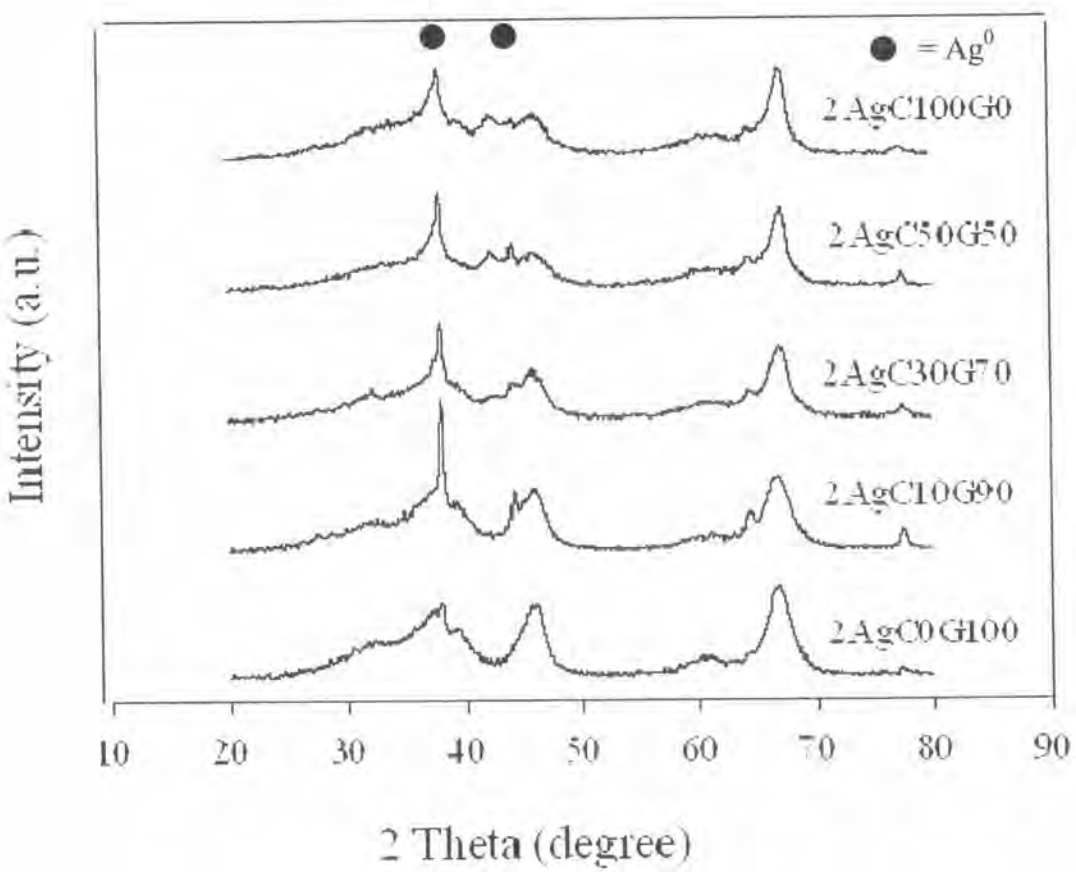

Figure 5.5 XRD patterns of 2 wt% Ag on alumina supports

5.2.3 XPS

Because of its surface sensitivity, XPS is used to identify the surface compositions of the catalysts as well as the interaction between metal and the supports. The results are given in table 5.4. It was found that the binding energy values of each sample were not change and these values were similar to the values from other researchers [167-173]. The atomic concentration ratios of Al/O in the pure gamma and pure chi alumina were the same value but they were different from the value of the mixed phase. XPS analysis revealed an increasing Ag surface concentration with increasing amount of chi phase. M. Richter et al. [173] reported that the size of the Ag clusters was larger than the penetration depth of the photo electrons and concluded that not all of the silver inside the clusters was detected by XPS. This leaded to the low Ag/Al atomic ratio. The lower ratio showed that the metal size was large. Such results suggested weaker interaction between Ag and alumina support because of higher metallic Ag agglomeration. The results of Pt/Al_2O_3 can not determine by the XPS because the platinum loading was low.

Table 5.4 Surface compositions by XPS of 2 wt% Ag/Al_2O_3.

Sample	Binding energy (eV)			Atomic concentration (%)	
	O 1s	Ag $3d_{5/2}$	Al 2p	Al/O	Ag/Al
Ag/C0G100	533.1	369.8	75.8	0.56	0.015
Ag/C10G90	533.1	369.8	75.8	0.48	0.015
Ag/C30G70	533.1	369.7	75.8	0.53	0.014
Ag/C50G50	533.1	369.6	75.8	0.54	0.041
Ag/C100G0	533.1	369.8	75.9	0.56	0.021

5.2.4 Catalytic activity

The selective catalytic reduction of NO by propane was carried out in fixed-bed quartz reactor under different reaction conditions in order to determine the catalytic activity of the catalysts. The results of this reaction showed in terms of temperature profile of NO conversion to N_2 and C_3H_6 conversion as Figures 5.6 and 5.7, respectively. The catalytic activity of the 10% chi phase showed higher NO conversion than gamma alumina phase. The reaction mechanism depended on the types of Ag phase, as proposed by Meunier et al [174]. The large Ag^0 likely observed on high silver loading, could promote the decomposition reduction of NO. In this work, the mixed phase of the gamma and chi alumina showed the formation of Ag^0 in the low loading because of the effect of interaction between metal and support. The large Ag^0 in 10 wt% chi phase improved activity of the silver catalyst and restrained the formation of the N_2O at low loading. The increase of the chi phase affected the higher temperature of the NO conversion to N_2, which may be the acidity of the alumina supported. The acidity of the alumina supports was shown in Figure 5.4. The chi alumina phase had higher acidity than gamma alumina phase.

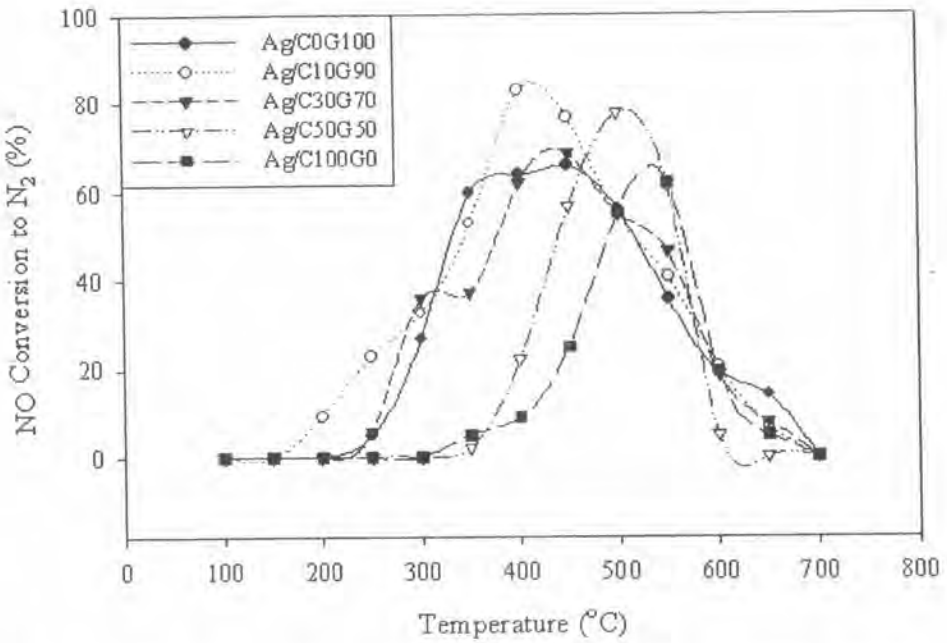

Figure 5.6 NO conversion to N_2 profiles of 2 wt% Ag/Al_2O_3 for SCR of NO by propene under lean-burn condition.

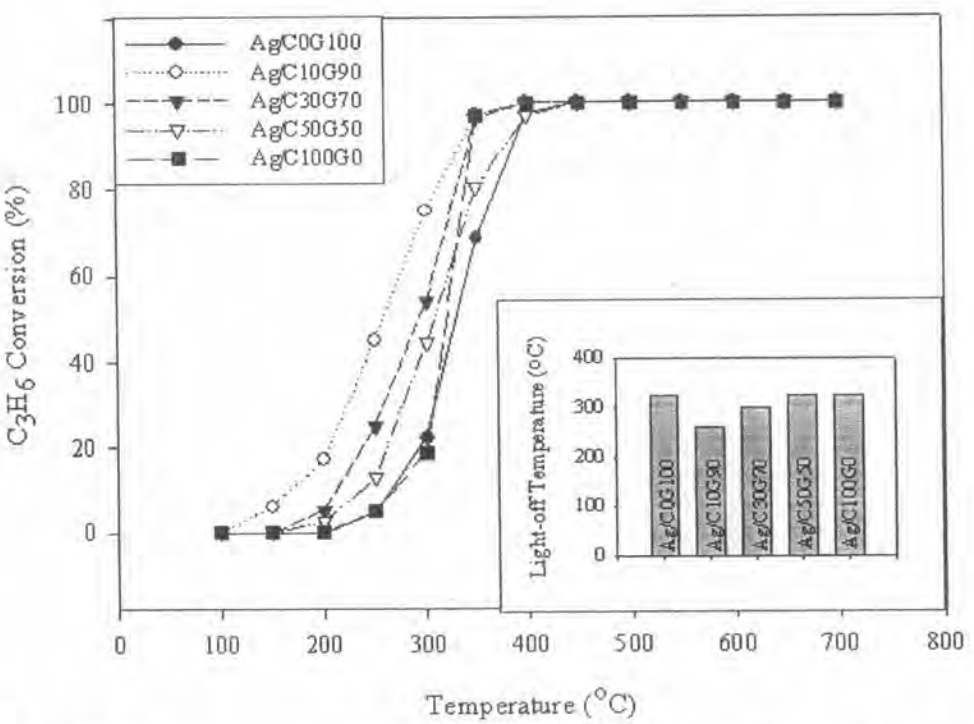

Figure 5.7 C_3H_6 conversion profiles of 2 wt% Ag/Al_2O_3 for SCR of NO by propene under lean-burn condition.

5.3 Carbon monoxide oxidation

The aluminas with various phase compositions were used as the catalyst support. The platinum was impregnated on them at about 0.3 wt%.

5.3.1 Physical properties of 0.3 wt% Pt/Al_2O_3

The results are given in table 5.5. The BET surface areas of the alumina supported Pt catalysts were slightly less than those of the original alumina supports. This indicated plugging of the loaded platinum on some of the alumina pores. After loading the Pt, decrease of the BET surface area with increasing the fraction of chi phase was observed similar to behavior of the unloaded alumina support. The metal active sites on the aluminas with pure phase were rather equivalent at approximately 3.2×10^{18} molecule $CO\cdot(g\ catalyst)^{-1}$. The mixed phase aluminas can assist high dispersion of platinum on them except the 10% chi phase. Surprisingly, the metal dispersion was maintained constant in a wide range between 30 and 70% chi phase composition. This phenomenon can be useful for the insensitive-structure reaction. However, a low content of the chi phase in the alumina could promote formation of larger platinum particle size. This effect was also observed on the other metal oxides. Panpranot et al. [175] have studied effect of the phase composition of TiO_2 on the amount of palladium active sites. They reported that when the rutile phase of TiO_2 was increased, the amount of chemisorbed CO decreased.

Table 5.5 Catalyst properties of 0.3 wt% Pt/Al_2O_3

Sample	BET surface area ($m^2.g^{-1}$)	CO chemisorption x 10^{-18} (molecule CO.(g catalyst)$^{-1}$)	% Pt dispersion (%)	Metal size* (nm)
Pt/C0G100	203	3.25	39	3
Pt/C10G90	195	2.53	30	4
Pt/C30G70	189	3.56	43	3
Pt/C50G50	177	3.55	43	3
Pt/C70G30	163	3.58	43	3
Pt/C100G0	151	3.18	38	3

* Calculate from CO chemisorption

5.3.2 X-ray diffraction pattern

XRD pattern of the alumina supports is shown in Figure 5.8. For the pure gamma phase, XRD peaks at 32°, 37°, 39°, 45°, 61° and 66° were evident. When adding toluene in 1-butanol, XRD peaks were appeared at 37°, 40°, 43°, 46°, 60°, and 67°. The peak at 43° was dominant. This peak showed characteristics of the chi phase and thus the increase of % chi alumina phase leaded to larger peak area at 43°. Certainly, the pure gamma alumina did not show the peak area at 43°. The peak of platinum oxide can not be observed by the XRD pattern because the XRD can not detect the particle size smaller than 3 nm.

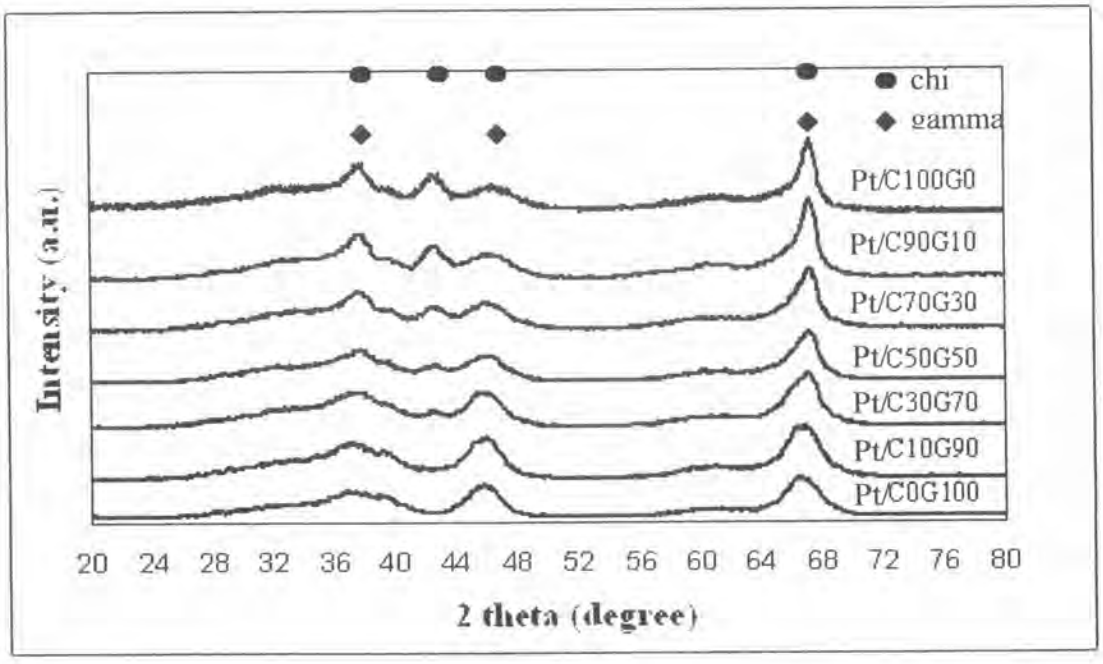

Figure 5.8 XRD patterns of 0.3 wt% Pt/Al_2O_3

5.3.3 EDX

The EDX shows well dispersion of Pt, Ag and O element of the sample. To confirm the presence of the PtO_xCl_y species on the catalyst surface, the amount of Cl was determined by EDX technique. EDX results showed no Cl element in every catalyst samples. The EDX spectrum is shown in Figure 5.9(a)-(f).

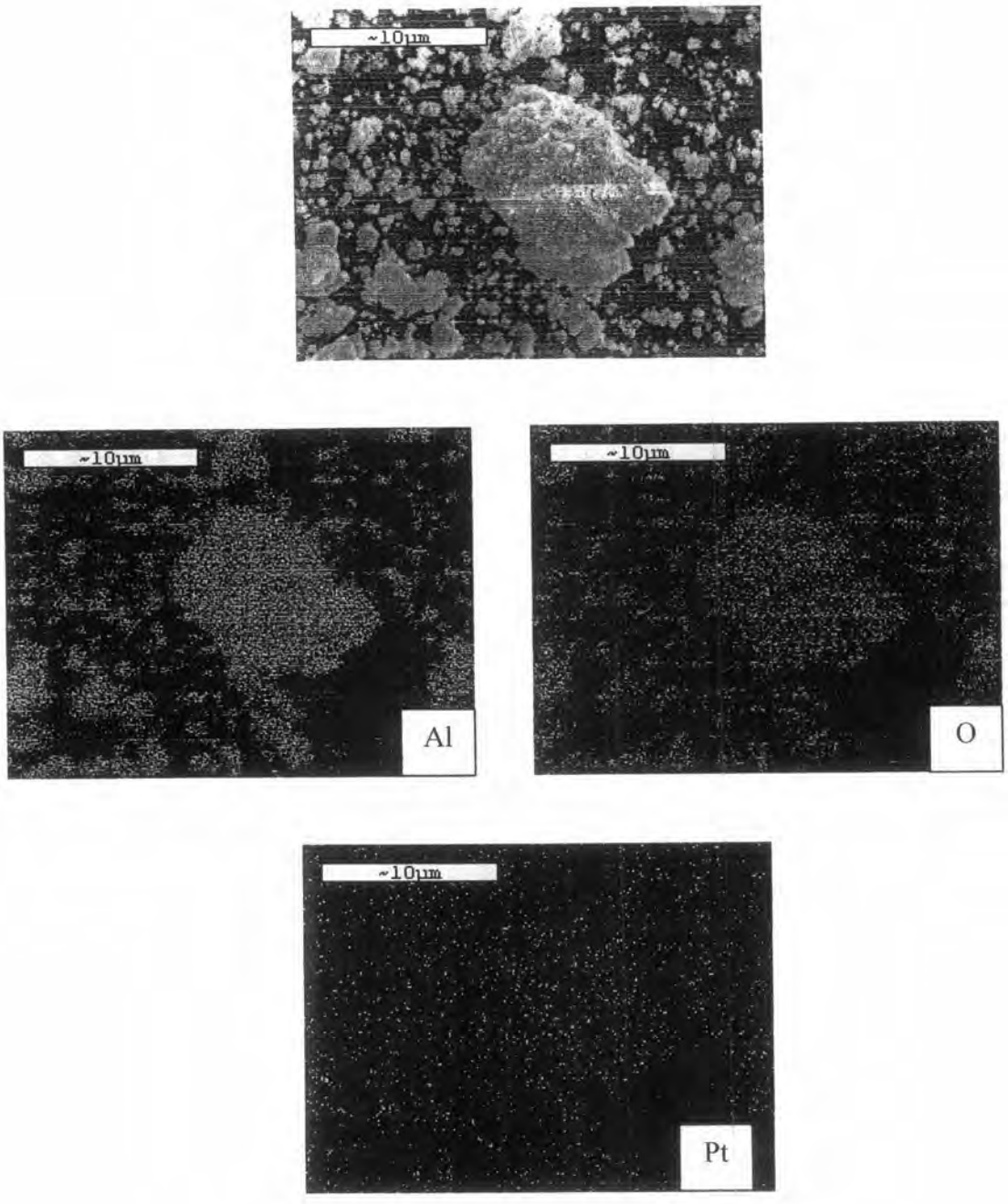

Figure 5.9(a) EDX micrograph of Pt/C0G100

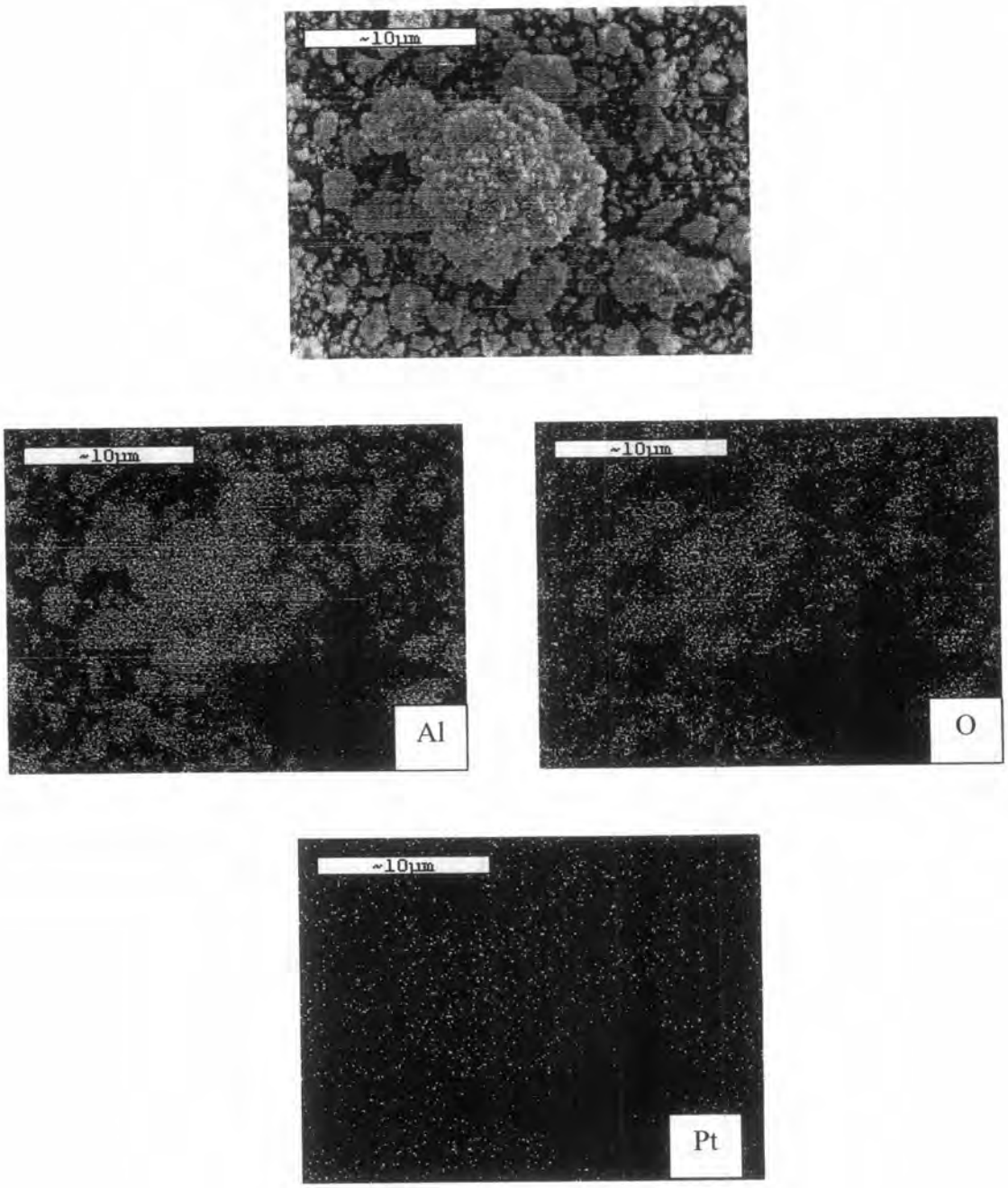

Figure 5.9(b) EDX micrograph of Pt/C10G90

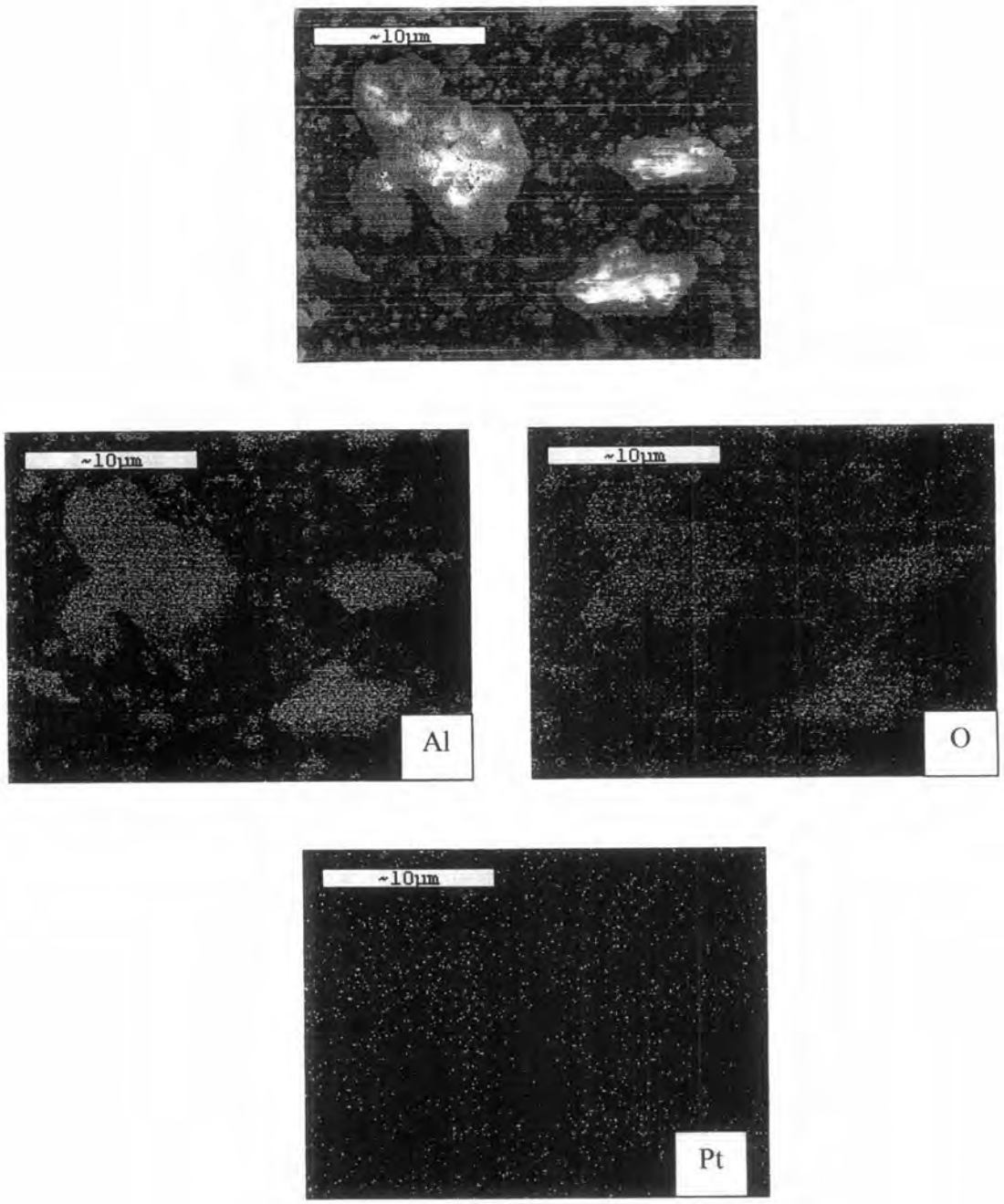

Figure 5.9(c) EDX micrograph of Pt/C30G70

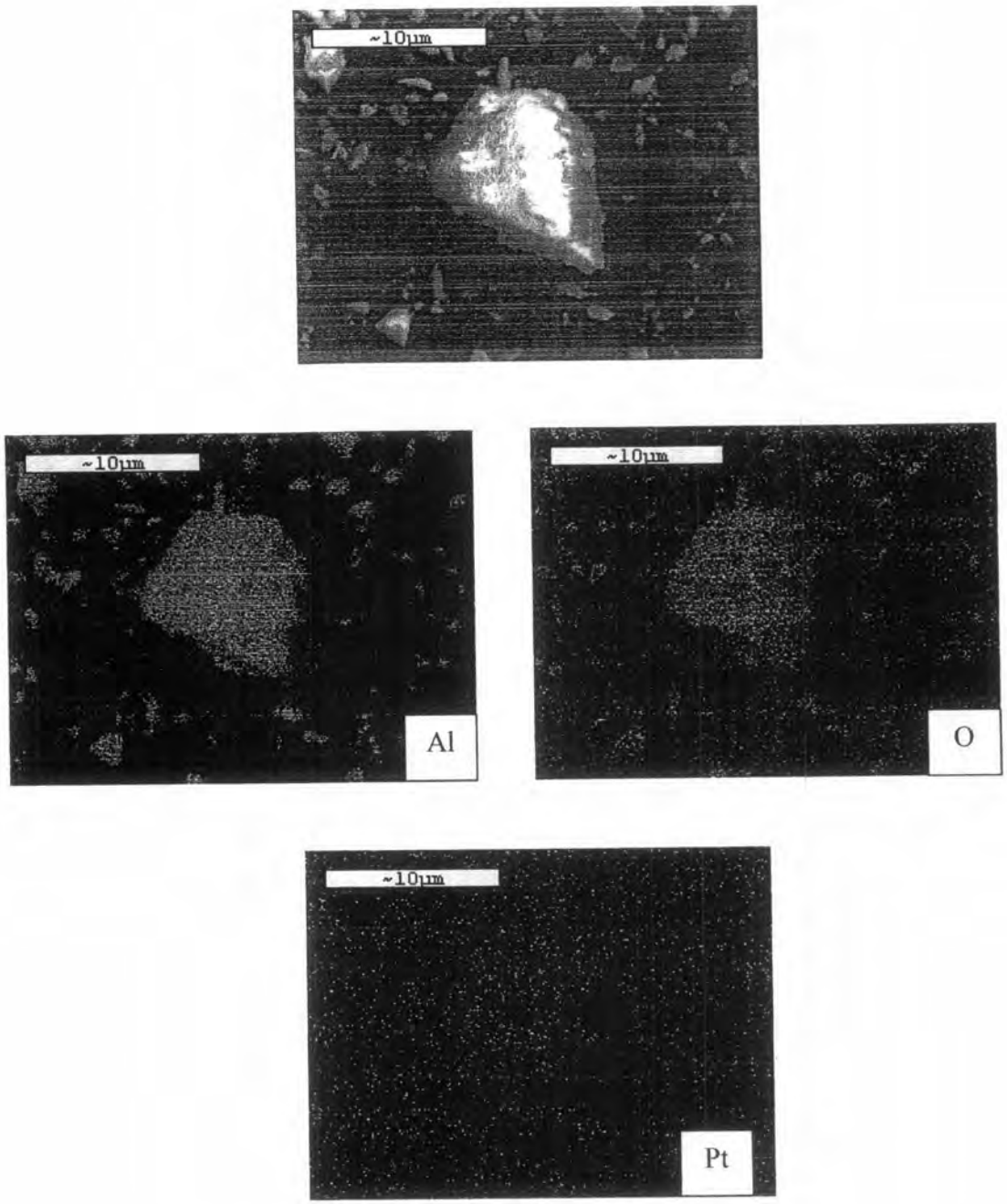

Figure 5.9(d) EDX micrograph of Pt/C50G50

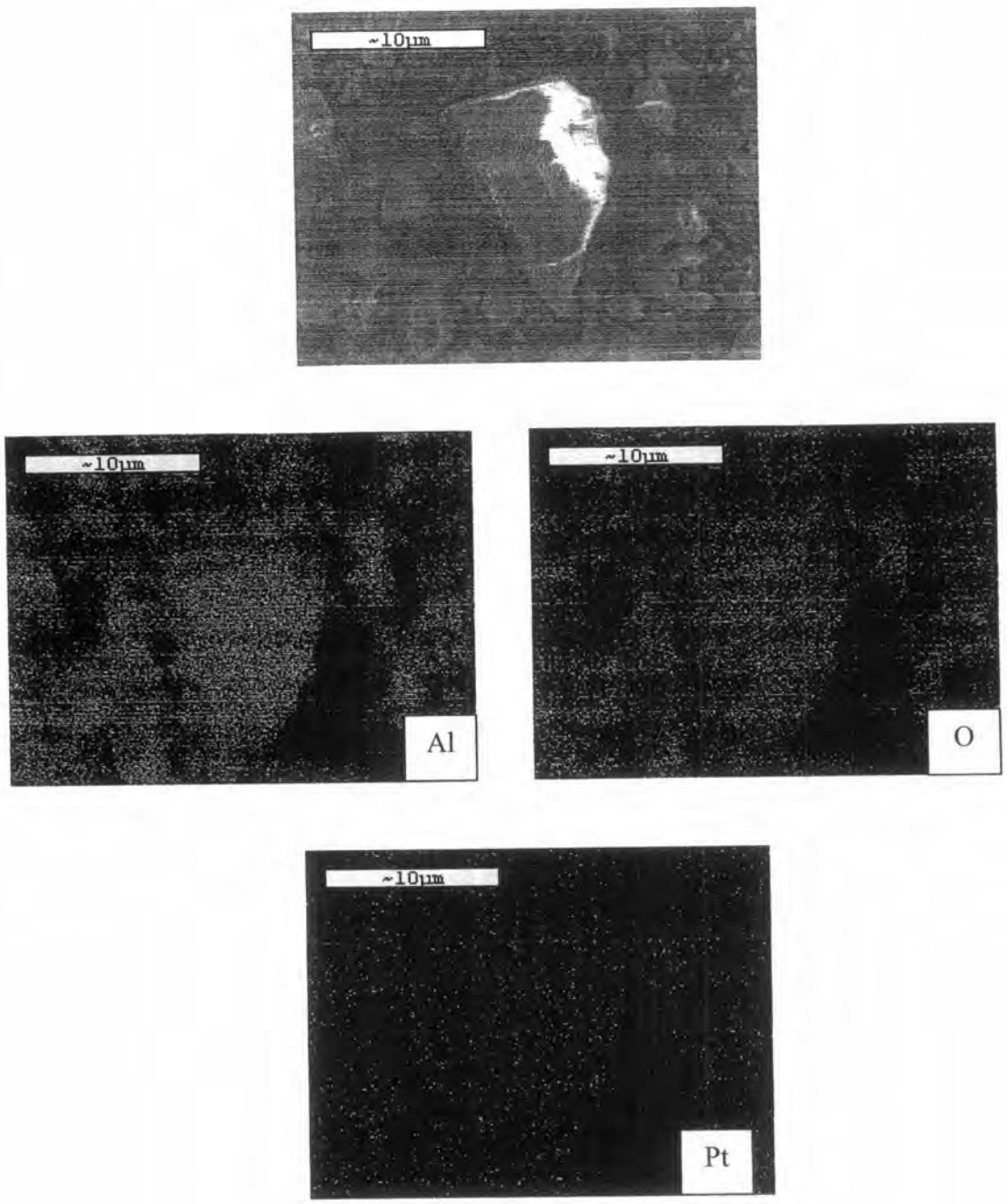

Figure 5.9(e) EDX micrograph of Pt/C70G30

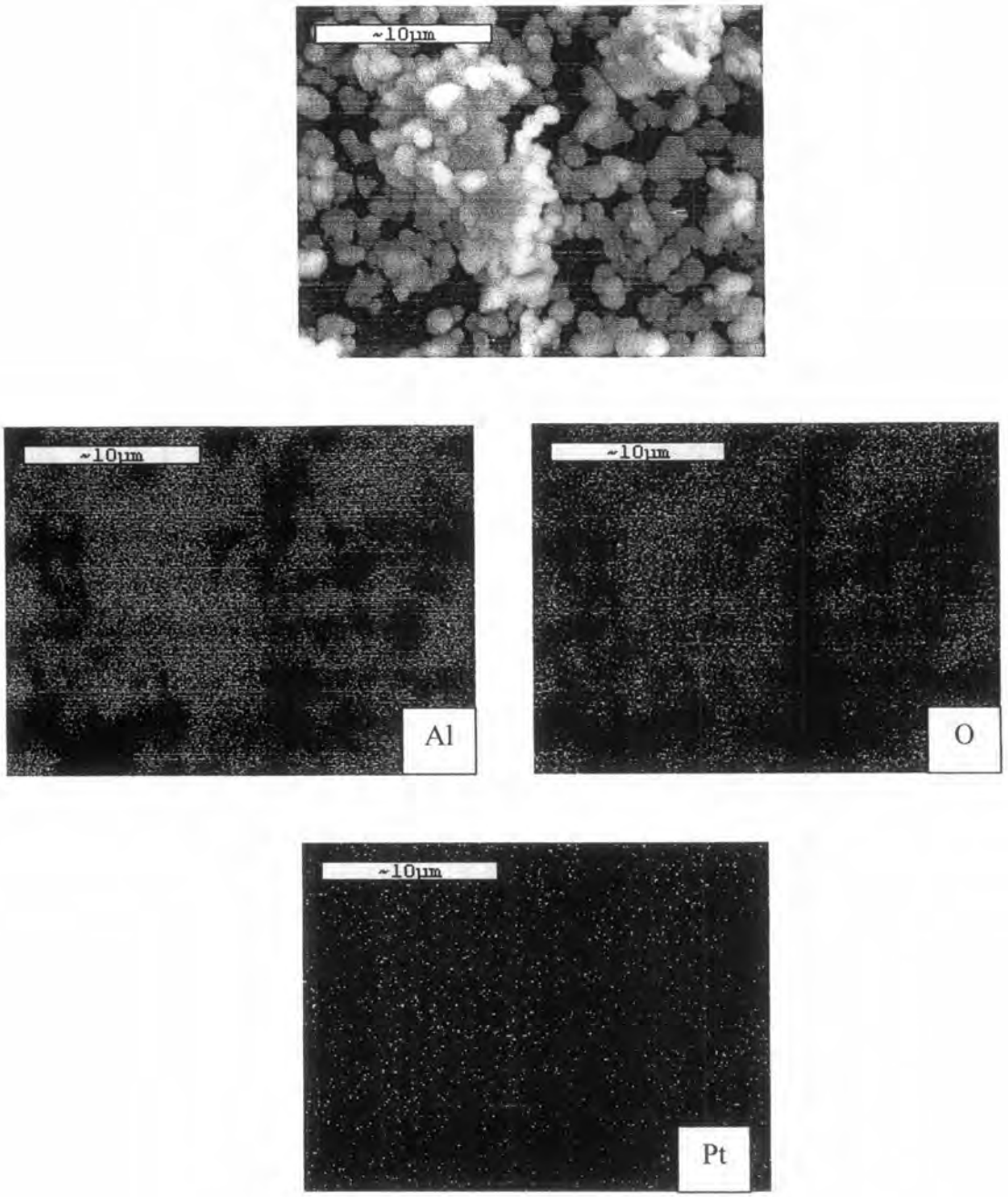

Figure 5.9(f) EDX micrograph of Pt/C100G0

5.3.4 Temperature programmed reduction

Temperature programmed reduction (TPR) is a powerful tool to study the reduction behavior of the catalysts. The TPR profiles of various chi/gamma phase compositions of alumina supported platinum catalysts are shown in Figure 5.9. The TPR profiles of platinum species were rather complex. They indicated differences in the interaction between the platinum species and the supports. All the catalyst samples exhibited two main reduction regions in ranges of 200-300 and 400-500 °C. Navarro et al. [176] found two main reduction peaks at 110 and 239 °C and a minor peak at 377 °C over 0.75 wt% Pt/Al_2O_3. They pronounced that the low-temperature peak, only observed for this platinum-supported sample, was assigned to the reduction of PtO_2 species [176,177] and the peaks at 239 and 377 °C were attributed to oxychlorinated species in the bulk and two-dimensional phase, with a strong interaction with alumina, respectively [176-178].

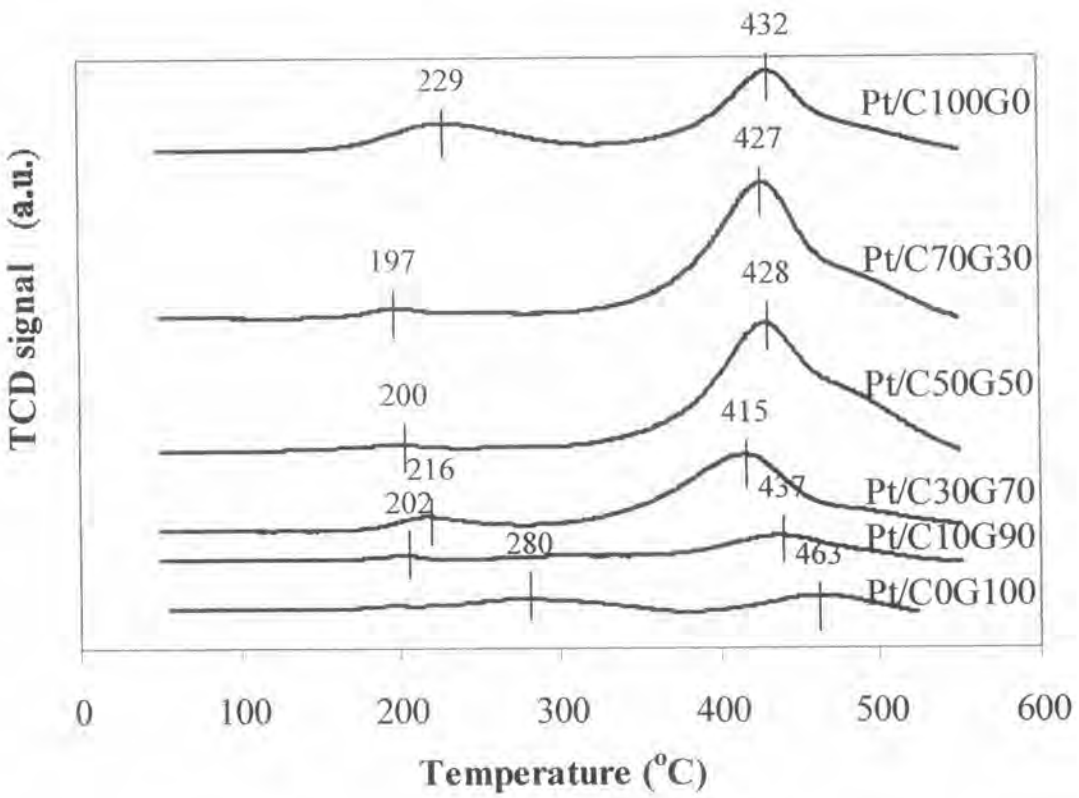

Figure 5.10 Temperature programmed reduction profiles of 0.3 wt% Pt/Al_2O_3

Therefore, all of the TPR profiles did not show the reduction of the PtO_xCl_y species. Both of the reduction peaks were assigned to the reduction of PtO_x species. The 200-300 °C peaks were bulk phase of the PtO_x while the 400-500 °C peaks were addressed as its strong interaction dispersive phase. This speculation was agreement with some literature [179, 180]. Tiernan et al. [179] found two reduction peaks at 220 and 420 °C over Pt/Al_2O_3. Two reduction peaks were assigned to the reduction of dispersed PtO_x. Santos et al. [180] reported that the TPR profile of Pt/Al_2O_3 sample showed two peaks at 287 and 434 °C. They pronounced that the peak at 287 °C was assigned to a reduction of Pt-oxide species and/or to a reduction of oxychlorplatinum surface complex $[PtO_xCl_y]_s$. From the section 5.3.3, the EDX results showed no Cl element in every catalyst sample. Therefore, all of the TPR profiles did not show the reduction of the PtO_xCl_y species. Both of the reduction peaks were assigned to the reduction of PtO_x species. The peak at 434 °C was assigned to a reduction of dispersed Pt in isolated patches PtO_x on alumina. From the Figure 5.9, the presence of the chi phase in the γ-Al_2O_3 can lower the reduction temperature of PtO_x species. The amount of H_2 consumption for each sample ia different as shown in table 5.6. It was significantly larger when the chi phase composition exceeded 30%, especially at 50 and 70% of chi phase. This implied a high chemical stoichiometric value of O/Pt in PtO_x complex or formation of $PtAl_2O_4$ spinal species [181]. Effect of the phase composition on the reduction characteristics on the other catalysts was also reported in the literature [182]. Jongsomjit et al. [182] have studied cobalt dispersion on TiO_2 and found that the presence of 19% rutile phase in titania facilitated the reduction of highly dispersed cobalt oxide to cobalt metal.

Table 5.6 The H_2 volume of the reduction peaks.

Sample	Temperature (°C) at peak	H_2 volume (ml/g)	N_O/N_{Pt}
Pt/C0G100	280	0.15	0.8
	463	0.16	
Pt/C10G90	202	0.02	0.7
	437	0.24	
Pt/C30G70	216	0.07	1.7
	415	0.59	
Pt/C50G50	200	0.05	2.8
	428	1.01	
Pt/C70G30	197	0.05	2.8
	427	1.02	
Pt/C100G0	229	0.22	2.0
	432	0.55	

5.3.5 Catalytic activity

CO oxidation was carried out as an insensitive-structure probe reaction to determine the catalytic activity of the catalyst samples. The results are shown in Figure 5.11. As expected, the CO oxidation activities were followed by the amount of platinum active sites. The presence of 30-70% chi phase composition can lower the light-off temperature by 15 °C. On the other hand, the 10% chi phase showed the worst catalytic activity in this reaction. These results can confirm CO chemisorption measurement as well.

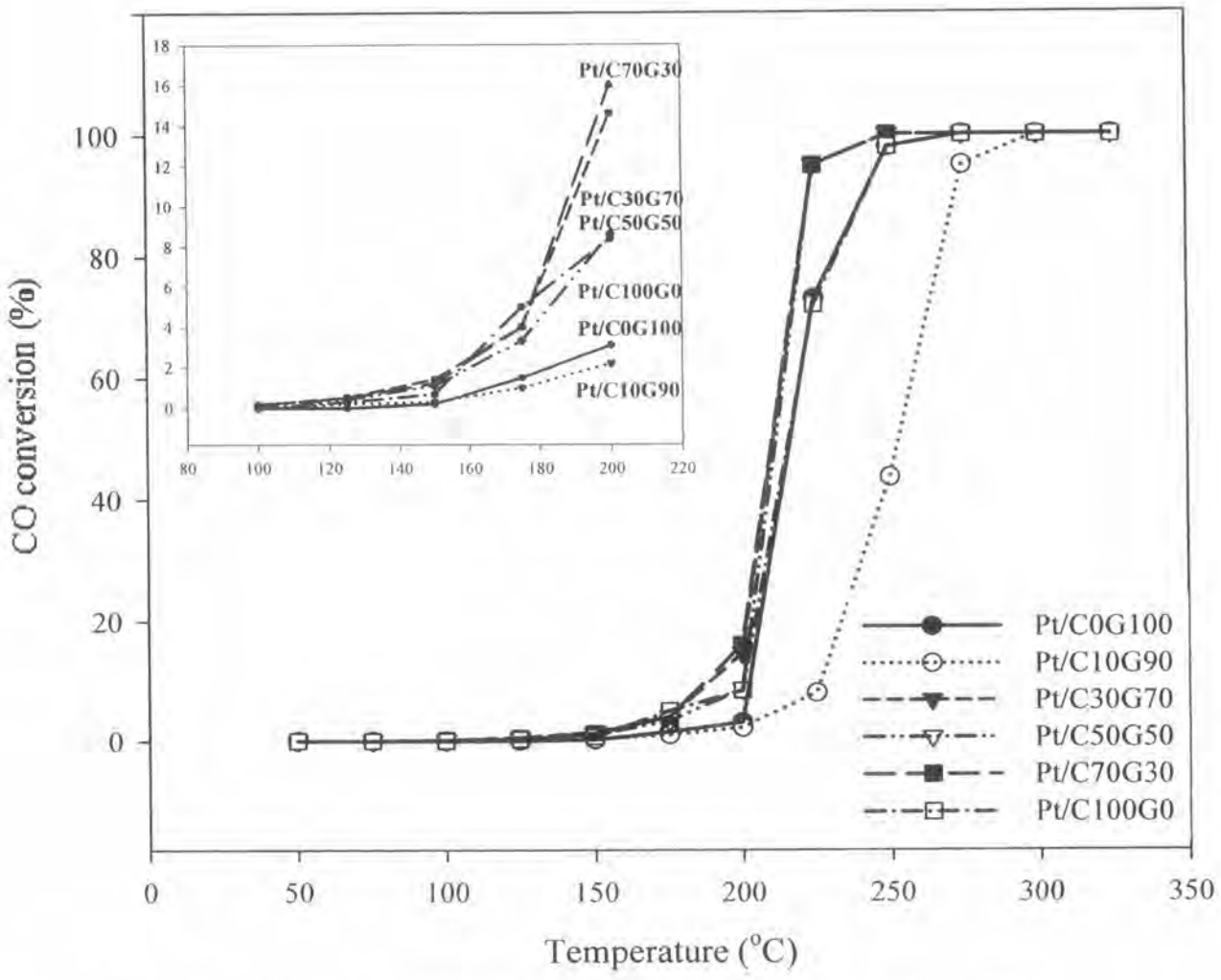

Figure 5.11 CO conversion profiles of 0.3 wt% Pt/Al_2O_3 for the CO oxidation

5.4 Selective carbon monoxide oxidation

The platinum was impregnated on the alumina supports with 0.3 and 1 wt% loading. In this work, the 0.3 wt% and 1 wt% platinum on the gamma alumina support were called 0.3Pt/C0G100 and 1Pt/C0G100 while those on the chi alumina support were called 0.3Pt/C100G0 and 1Pt/C100G0, respectively.

5.4.1 Physical properties of 0.3 wt% and 1 wt% Pt/Al_2O_3

The properties of the samples are summarized in table 5.7. The BET surface area of the gamma and chi alumina showed 226 and 168 m^2/g. The BET surface areas of the alumina supported Pt catalysts were slightly less than those of the original alumina supports. After loading Pt, a decrease of the BET surface area with increasing the fraction of chi phase was observed similar to the behavior of the unloaded alumina support. For both platinum loading, the metal active sites on the gamma and chi phase were rather equivalent.

Table 5.7 Catalyst properties of the Pt/Al_2O_3

Sample	BET surface area ($m^2 \cdot g^{-1}$)	Metal active sites $\times 10^{-18}$ (molecule CO/g catalyst)	Pt dispersion (%)	Matel size* (nm)
gamma alumina	226	-	-	-
chi alumina	168	-	-	-
0.3Pt/C0G100	203	3.24	38	3
0.3Pt/C100G0	151	3.18	38	3
1Pt/C0G100	189	10.8	39	3
1Pt/C100G0	133	11.5	40	3

* Calculate from CO chemisorption

5.4.2 X-ray diffraction pattern

XRD profiles of the alumina supports and catalyst samples are shown in Figure 5.12. The XRD of catalyst sample shows the same trend as the alumina sample. The XRD program reference (PCPDFWIN) showed the main peak of PtO at 33.5°, 54.3°,60° and 70.6°, the PtO_2 at 28°, 34.8° and 54°, the Pt_3O_4 at 22.5°, 36°, 57° and 59°. The peak of platinum oxides was not observed because of the XRD can not detect the metal size less than 3 nm.

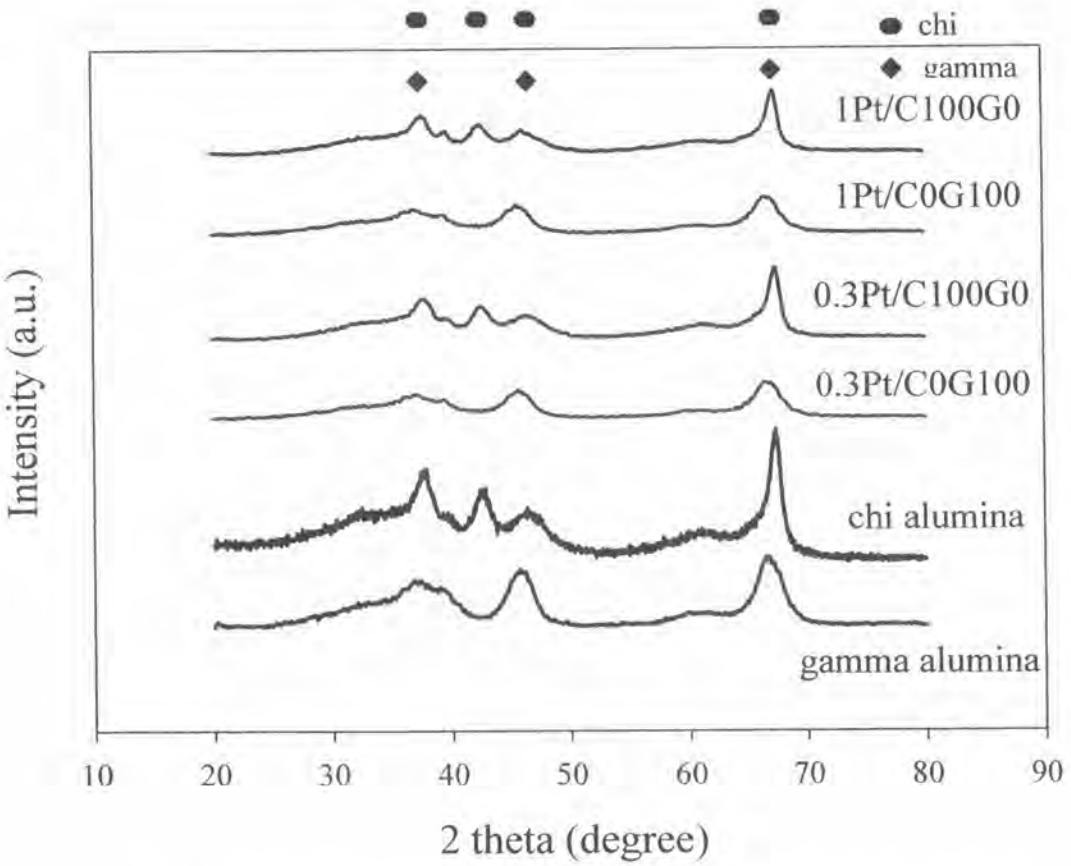

Figure 5.12 XRD patterns of alumina supports and Pt/Al_2O_3 catalysts

5.4.3 Temperature programmed reduction

From the Figure 5.13, platinum oxide on chi alumina show higher reducibility than that on gamma alumina. The difference in reducibility may be caused by the different form of platinum oxide on the supports, which can be confirmed by TPR results. The peak in range of 100-200 °C was observed in higher platinum loading. Navarro et al. [176] reported that this peak was assigned to the PtO_2 species. The two peaks in range of 200-300 and 400-500 °C were found in all the catalyst samples. From the result, the high platinum loading had weak interaction of PtO_2 with alumina but did not have it in the low loading.

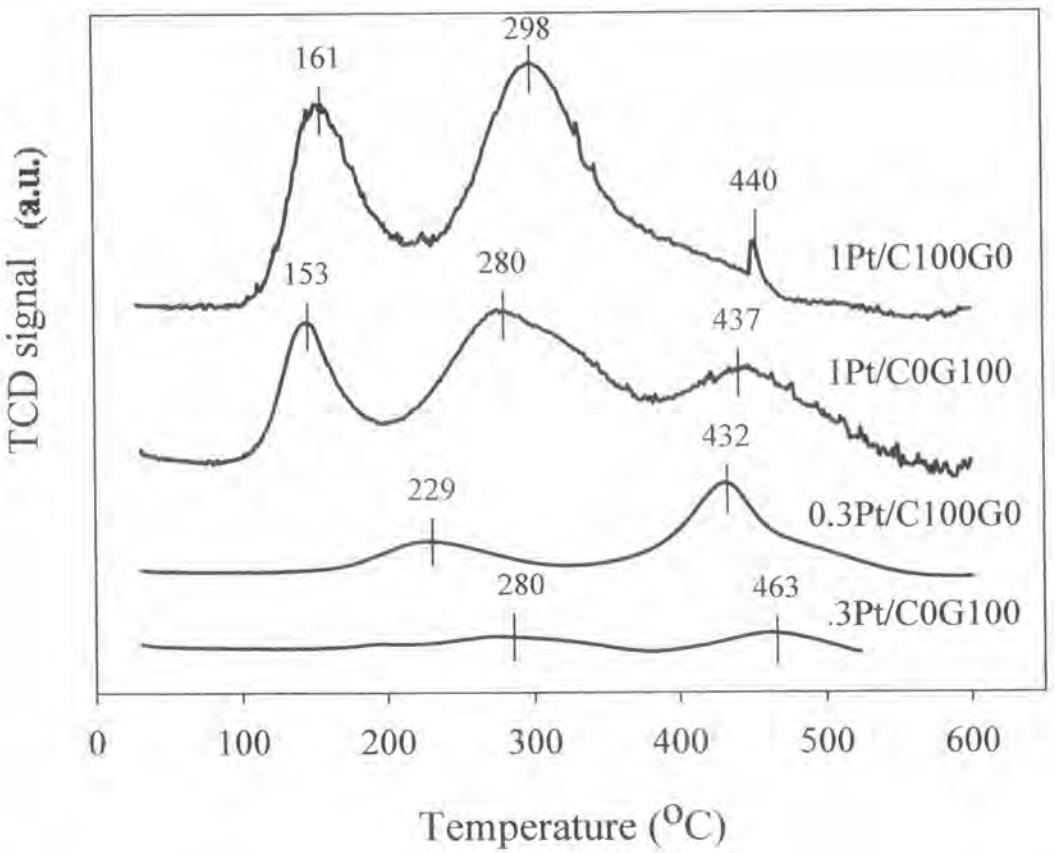

Figure 5.13 Temperature programmed reduction profiles of platinum catalysts

5.4.4 Temperature programmed desorption of carbon monoxide

The CO-TPD spectra of the Pt/Al_2O_3 catalysts are given in Figure 5.14. The peak at low temperatures was observed in the high platinum loading. The position of CO desorption peak shifted to higher temperatures in the gamma alumina supported.

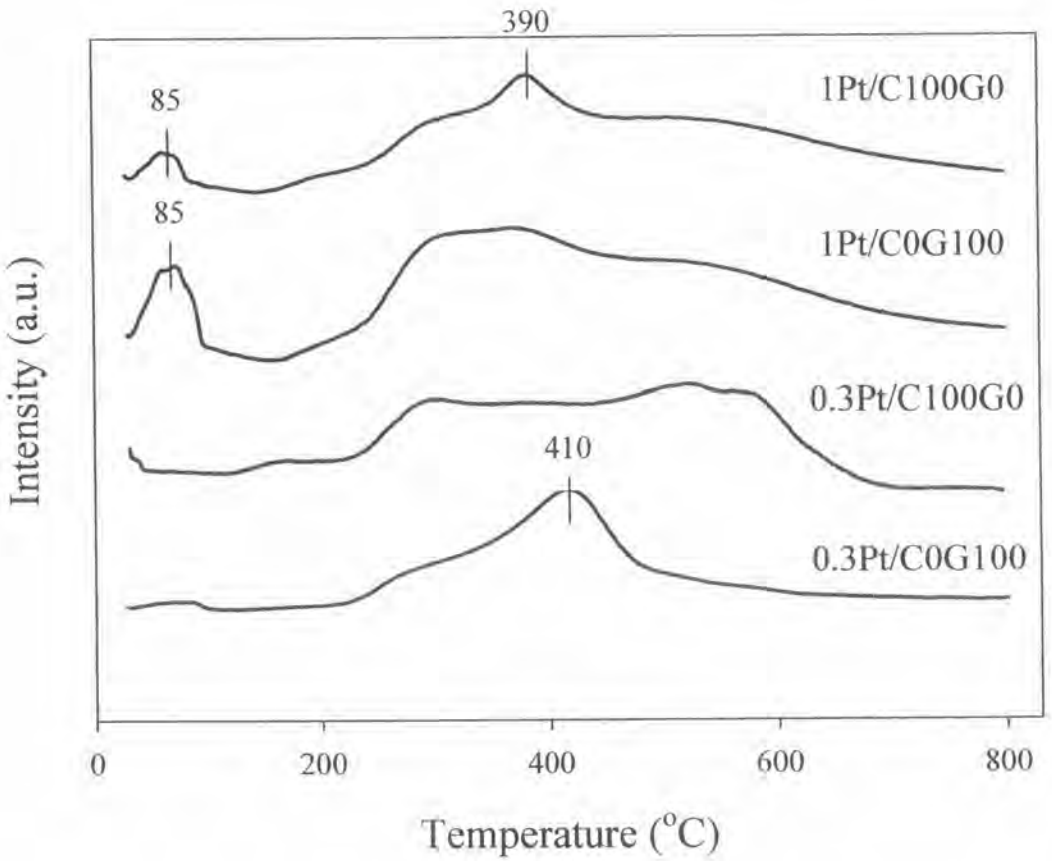

Figure 5.14 CO-temperature programmed desorption profiles of platinum catalysts

5.4.5 Temperature programmed desorption of hydrogen

The H_2-TPD spectra of the Pt/Al_2O_3 catalysts are given in Figure 5.15. The position of H_2 desorption peak of chi alumina shifted to lower temperature than gamma alumina.

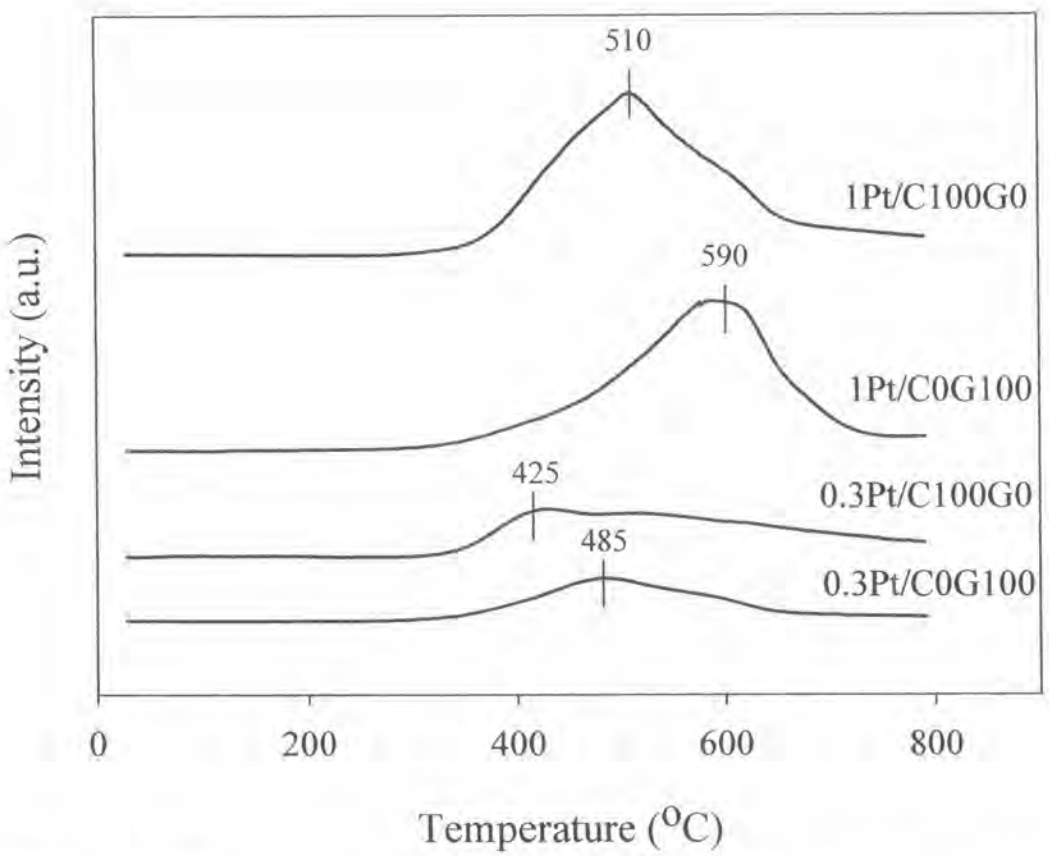

Figure 5.15 H_2-temperature programmed desorption profiles of platinum catalysts

5.4.6 Catalytic activity

The catalytic activity of Pt/Al_2O_3 catalysts for selective CO oxidation was investigated. The CO conversion and selectivity of various catalysts are shown in Figures 5.16 and 5.17. The catalytic performance of platinum catalysts can be improved by chi alumina. The 0.3 wt% Pt/χ-Al_2O_3 catalyst exhibited high catalytic activity with low light-off temperature of CO conversion at 150 °C and with selectivity to CO_2 around 80% at 125 °C. Obviously, the catalytic performance of the Pt supported on chi alumina was higher than that supported on gamma alumina. This can be explained by TPR results that H_2 consumption of the Pt/χ-Al_2O_3 catalyst was higher than that of the Pt/γ-Al_2O_3 catalyst. It implied higher reducibility and more oxygen surface coverage on chi alumina. The results showed the same trend with literature. Sirichaiprasert et al. [183] studied the catalytic performance of Cu–Ce–Fe–O composite-oxide and found that the O_2 pretreated catalyst gave higher performance than that obtained from H_2 pretreated catalyst and non-pretreated catalyst, respectively. O_2 pretreatment enhances the O_2 adsorption on Cu active species and then virtually form CuO active species on the catalyst for selective CO oxidation [184-186]. Thus, CuO active species of the catalyst are improved by O_2 pretreatment. It is known that high oxygen storage capacity of reducible oxides improves catalytic performance by storing oxygen during oxidation and releasing it during reduction [187, 188]. Hanbo Zou et al. [189] found the activity of selective CO oxidation decreases when the peak of CO-TPD shifted to higher temperature.

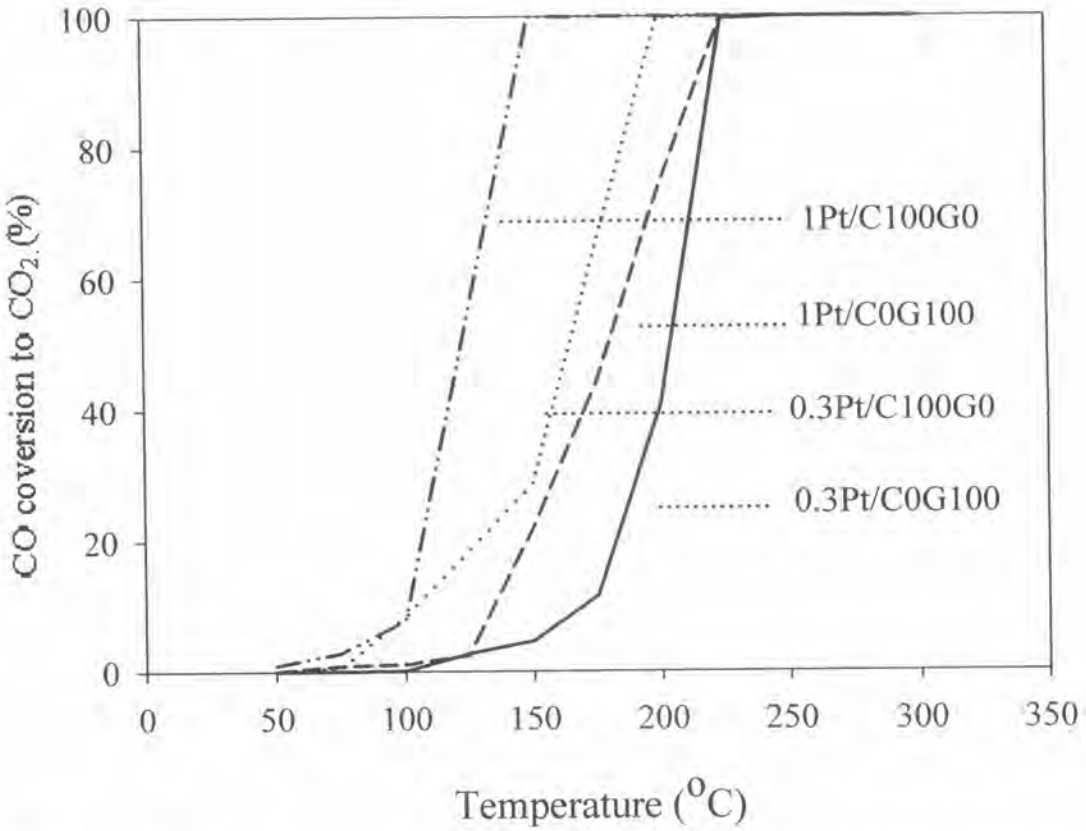

Figure 5.16 The CO conversion profiles of Pt/Al_2O_3 for selective CO oxidation

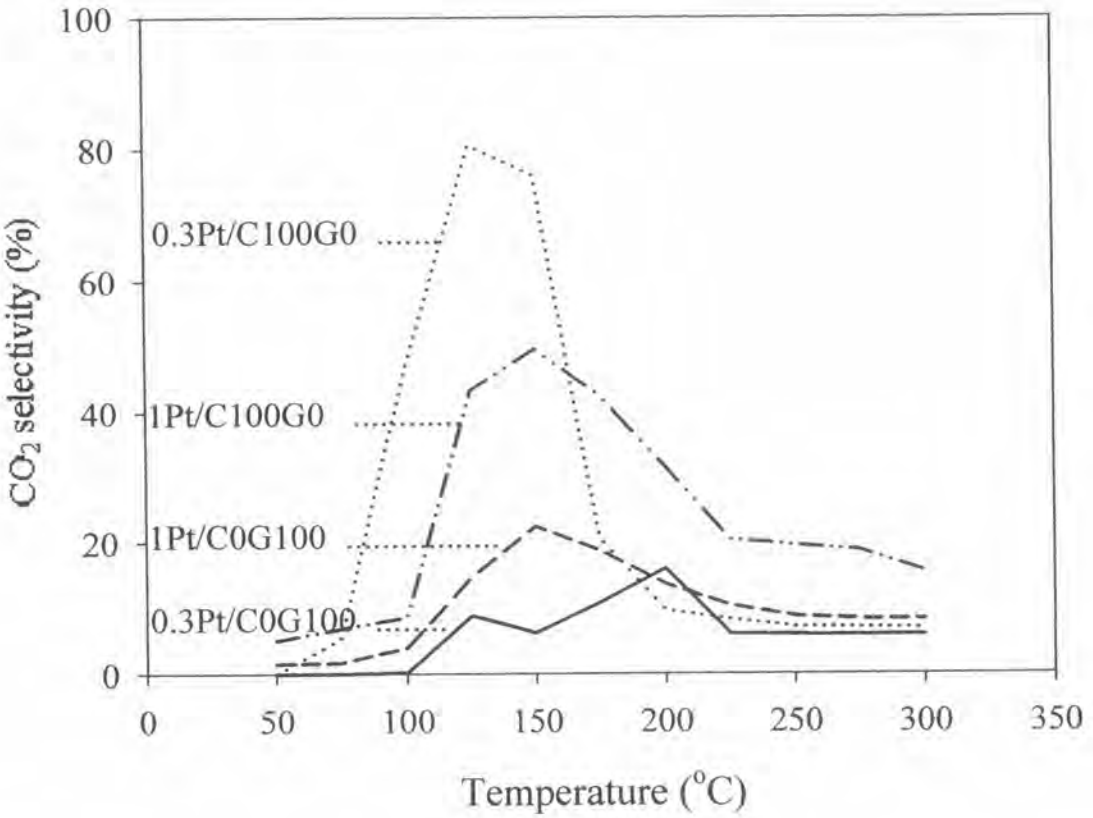

Figure 5.17 The CO_2 selectivity profiles of Pt/Al_2O_3 for selective CO oxidation